Atmos. Chem. Phys. Discuss., 14, 1073–1112, 2014
www.atmos-chem-phys-discuss.net/14/1073/2014/
doi:10.5194/acpd-14-1073-2014

Atmospheric Chemistry and Physics Discussions
Open Access

Evidence for an earlier greenhouse cooling effect in the stratosphere before the 1980s over the Northern Hemisphere

C. S. Zerefos[1,2], K. Tourpali[3], P. Zanis[4], K. Eleftheratos[5], C. Repapis[1,10], A. Goodman[6], D. Wuebbles[7], I. S. A. Isaksen[8], and J. Luterbacher[9]

[1]Research Centre for Atmospheric Physics and Climatology, Academy of Athens, Athens, Greece
[2]Navarino Environmental Observatory (N.E.O.), Messinia, Greece
[3]Laboratory of Atmospheric Physics, Department of Physics, Aristotle University of Thessaloniki, Thessaloniki, Greece
[4]Department of Meteorology and Climatology, School of Geology, Aristotle University of Thessaloniki, Thessaloniki, Greece
[5]Laboratory of Climatology & Atmospheric Environment, University of Athens, Greece
[6]Department of Atmospheric Science, Colorado State University, Fort Collins, CO, USA
[7]Department of Atmospheric Sciences, University of Illinois, Urbana, IL, USA
[8]Department of Geosciences, University of Oslo, Oslo, Norway
[9]Climatology, Climate Dynamics and Climate Change, Department of Geography, Justus-Liebig University of Giessen, Germany

[10]Mariolopoulos-Kanaginis Foundation for the Environmental Sciences, Athens, Greece

Received: 5 November 2013 – Accepted: 29 December 2013 – Published: 14 January 2014

Correspondence to: C. S. Zerefos (zerefos@geol.uoa.gr)

Published by Copernicus Publications on behalf of the European Geosciences Union.

ACPD
14, 1073–1112, 2014

Evidence for an earlier greenhouse cooling effect

C. S. Zerefos et al.

Abstract

This study provides a new look at the observed and calculated long-term temperature changes since 1958 for the region extending from the lower troposphere up to the lower stratosphere of the Northern Hemisphere. The analysis is mainly based on monthly layer mean temperatures derived from geopotential height thicknesses between specific pressure levels. Layer mean temperatures from thickness improve homogeneity in both space and time and reduce uncertainties in the trend analysis. Datasets used include the NCEP/NCAR I reanalysis, the Free University of Berlin (FU-Berlin) and the RICH radiosonde datasets as well as historical simulations with the CESM1-WACCM global model participating in CMIP5. After removing the natural variability with an autoregressive multiple regression model our analysis shows that the time interval of our study 1958–2011 can be divided in two distinct sub-periods of long term temperature variability and trends; before and after 1980s. By calculating trends for the summer time to reduce interannual variability, the two periods are as follows. From 1958 until 1979, non-significant trends or slight cooling trends prevail in the lower troposphere ($0.06 \pm 0.06\,^{\circ}\mathrm{C\,decade}^{-1}$ for NCEP and $-0.12 \pm 0.06\,^{\circ}\mathrm{C\,decade}^{-1}$ for RICH). The second period from 1980 to the end of the records shows significant warming trends ($0.25 \pm 0.05\,^{\circ}\mathrm{C\,decade}^{-1}$ for both NCEP and RICH). Above the tropopause a persistent cooling trend is clearly seen in the lower stratosphere both in the pre-1980s period ($-0.58 \pm 0.17\,^{\circ}\mathrm{C\,decade}^{-1}$ for NCEP, $-0.30 \pm 0.16\,^{\circ}\mathrm{C\,decade}^{-1}$ for RICH and $-0.48 \pm 0.20\,^{\circ}\mathrm{C\,decade}^{-1}$ for FU-Berlin) and the post-1980s period ($-0.79 \pm 0.18\,^{\circ}\mathrm{C\,decade}^{-1}$ for NCEP, $-0.66 \pm 0.16\,^{\circ}\mathrm{C\,decade}^{-1}$ for RICH and $-0.82 \pm 0.19\,^{\circ}\mathrm{C\,decade}^{-1}$ for FU-Berlin). The cooling in the lower stratosphere is a persistent feature from the tropics up to 60 north for all months. At polar latitudes competing dynamical and radiative processes are reducing the statistical significance of these trends. Model results are in line with re-analysis and the observations, indicating a persistent cooling in the lower stratosphere during summer before and after the 1980s by $-0.33\,^{\circ}\mathrm{C\,decade}^{-1}$; a feature that is also seen throughout the year. However, the lower stratosphere modelled trends are generally lower than re-analysis and the observations. The contrasting effects of ozone depletion at polar latitudes in winter/spring and the anticipated strengthening of the Brewer Dobson circulation from man-made global warming at polar latitudes are discussed. Our results provide additional evidence for an early greenhouse cooling signal in the lower stratosphere before the 1980s, which it appears well in advance relative to the tropospheric greenhouse warming signal. Hence it may be postulated that the stratosphere could have provided an early warning of man-made climate change. The suitability for early warning signals in the stratosphere relative to the troposphere is supported by the fact that the stratosphere is less sensitive to changes due to cloudiness, humidity and man-made aerosols. Our analysis also indicates that the relative contribution of the lower stratosphere vs. the upper troposphere low frequency variability is important for understanding the added value of the long term tropopause variability related to human induced global warming.

1 Introduction

Since the discovery of the significant cooling trends in the lower stratosphere reported already by the late 1970s (Zerefos and Mantis, 1977; Angell and Korshover, 1983; Miller et al., 1992), a number of scientific articles have focused on the statistical space and time continuity of stratospheric temperature observations both from ground and from satellite retrievals. Those publications indicate that the lower stratosphere cooling continues from the 1980s to the present (Santer et al., 1999; Randel et al., 2009; WMO, 2011; Santer et al., 2013).

Common features in lower-stratospheric temperature change are found in all available radiosonde and satellite datasets[1]. One common finding is that in the global mean, the lower stratosphere has cooled by about -0.5° K decade^{-1} since 1980. Ran-

[1]Today, there are six available global lower-stratospheric temperature data sets based on radiosonde data since the late 1950s; RATPAC (Free et al., 2005); HadAT (Thorne et al.,

ACPD
14, 1073–1112, 2014

del et al. (2009) reported that lower stratosphere cooling is a robust result over much of the globe for the period 1979–2007, being nearly uniform over all latitudes outside of the polar regions, with some differences among the different radiosonde and satellite data sets. Substantially larger cooling trends are observed in the Antarctic lower stratosphere during spring and summer, in association with the development of the Antarctic ozone hole (Randel et al., 2009; Santer et al., 2013). In the tropical lower stratosphere the observations show significant long-term cooling over 70–30 hPa for 1979–2007, while less overall cooling is seen at 100 hPa (Randel et al., 2009). The global-mean lower stratospheric cooling has not occurred linearly, but stems from two downward steps in temperature, both of which are coincident with the cessation of transient warming after the volcanic eruptions of El Chichón and Mt. Pinatubo (Thompson and Solomon, 2009; Free and Lanzante, 2009). It should be also noted that the global mean lower stratospheric temperatures during the period following 1995 are significantly lower than they were during the decades prior to 1980, but have not dropped further since 1995 (WMO, 2011). Recently, Thompson et al. (2012) reported that the SSU data reprocessed by NOAA indicate stronger cooling trends in the middle and higher stratosphere than previously estimated, which cannot be captured by the available simulations with coupled chemistry–climate models (CCMs) and coupled atmosphere–ocean global climate models (AOGCMs). This global lower stratosphere cooling since the 1980s is also evident in the pre-satellite era with a cooling rate of $\sim 0.35\,\mathrm{K\,decade^{-1}}$ since 1958 (WMO, 2011). Randel et al., (2009) questioned the validity of the trends for the period 1958–1978 because of the sparse observational database and the known instrumental uncertainties for this period, together with the large trend uncertainties implied by the spread of results. Furthermore in other studies it was pointed that the radiosonde datasets are not fully independent and that there are systematic biases in a number of stations relative to the satellites (Randel and Wu, 2006; Free and Seidel,

2005); RATPAC-lite (Randel and Wu, 2006); RAOBCORE (Haimberger, 2007); RICH (Haimberger et al., 2008); and IUK (Sherwood et al., 2008) and three satellite datasets; UAH (Christy et al., 2003); RSS (Mears and Wentz, 2009); and STAR, (Zou et al., 2009).

ACPD
14, 1073–1112, 2014

2007). These systematic biases are not well understood. Nevertheless, the different statistical approaches applied for homogenization are useful to assessing the overall uncertainty of the long-term stratospheric temperature trend estimates since the late 1950s (WMO, 2011).

The primary radiative forcing mechanisms responsible for global temperature changes in the stratosphere since 1979 have been increases in well-mixed GHG concentrations, increases in stratospheric water vapour, the decrease in stratospheric ozone primarily related to chlorine and bromine from various halocarbons, the effects of aerosols from explosive volcanic eruptions, and the effects of solar activity changes (e.g., Shine et al., 2003; Ramaswamy et al., 2006; WMO, 2007; IPCC, 2007, 2013). The effects of volcanic eruptions, variations in solar radiation, and other sources of natural variability, including the wave-driven quasi-biennial oscillation (QBO) in ozone, can be accounted for through the use of indices in time series trends analyses (Tiao et al., 1990; Staehelin, 2001; Reinsel et al., 2005; Fioletov, 2009). However, the attribution of past lower stratosphere temperature trends is complicated by the effects of the increases and leveling off of ozone depleting substances (ODSs) and the low-frequency variability of the Brewer–Dobson (BD) circulation.

The expectation of an accelerated and stronger BD circulation in a warmer climate is consistent with results from transport chemistry climate model simulations, wherein the lower stratospheric temperature trends may result from increases in upwelling over the tropical lower stratosphere and strengthening of the BD circulation (Rind et al., 2001; Cordero and Forster, 2006; Butchart et al., 2006, 2010; Austin and Li, 2006; Rosenlof and Reid, 2008; Garcia and Randel, 2008; Lamarque and Solomon, 2010). Unfortunately the detection of trends in the BD circulation in observations is complicated because trends in BD circulation are small from 1980s through 2010 but are expected to become larger in the next few decades. In addition, the BD circulation is not a directly observed physical quantity (WMO, 2011). Yet, observational evidence of an accelerated BD has been shown in a number of studies over both the tropics (e.g., Thompson and Solomon, 2005; Rosenlof and Reid, 2008) and the high latitudes (Jo-

ACPD
14, 1073–1112, 2014

hanson and Fu, 2007; Hu and Fu, 2009; Lin et al., 2009; Fu et al., 2010). Thompson and Solomon (2009) have shown that the contrasting latitudinal structures of recent stratospheric temperature and ozone trends are consistent with the assumption of increases in the stratospheric overturning BD circulation. Also Free (2011) pointed out that trends in the tropical stratosphere show an inverse relationship with those over the Arctic for 1979–2009, which might be related to changes in stratospheric circulation. In contrast, other studies using derived quantities found no indication of an increasing meridional circulation (Engel et al., 2009) while Iwasaki et al. (2009) pointed that the yearly trends in BD strength, diagnosed from all re-analyses products over the common period 1979–2001, are not reliably observed due to large diversity among the reanalyses. According to Randel and Thompson (2011), since there are no direct measurements of upwelling near the tropical tropopause, and there are large uncertainties in indirect measurements or assimilated data products (Iwasaki et al., 2009), temperature and ozone observations at the tropics can provide a sensitive measure of upwelling changes in the real atmosphere. In a recent article, Kawatani, and Hamilton (2013) reported that a weakening trend in the lower stratosphere QBO amplitude provides strong support for the existence of a long-term trend of enhanced upwelling near the tropical tropopause.

The tropospheric warming and stratospheric cooling associated also with human forcing factors would influence their interface i.e. the tropopause region (Santer et al., 2003a; Santer et al., 2003b; Seidel and Randel, 2006; Son et al., 2009). Seidel and Randel (2006) examined global tropopause variability on synoptic, monthly, seasonal, and longer-term timescales using 1980–2004 radiosonde data and reported upward tropopause height trends at almost all of the (predominantly extratropical) stations analyzed, yielding an estimated global trend of $64 \pm 21\,\mathrm{m\,decade^{-1}}$. They reported that on multidecadal scale the tropopause height change is more sensitive to stratospheric temperature change than tropospheric change for both tropical and extratropical atmosphere and hence at the lowest frequencies the tropopause is primarily coupled with stratospheric temperatures. Furthermore, Son et al. (2009), who analysed a set of

ACPD
14, 1073–1112, 2014

Evidence for an earlier greenhouse cooling effect

C. S. Zerefos et al.

long-term integrations with stratosphere-resolving chemistry climate models, reported that at the northern mid-latitudes the long-term tropopause increase is dominated by the upper troposphere warming while over the tropics and the Southern Hemisphere extratropics, the long-term tropopause trend is almost equally affected by the lower stratosphere trend and upper troposphere warming.

A major open question that still remains to be answered is if the stratosphere can be considered as a more suitable region than the troposphere to detect anthropogenic climate change signals and what can be learned from the long-term stratospheric temperature trends? Indeed the signal-to-noise ratio in the stratosphere is more sensitive radiatively to anthropogenic GHGs forcing and less disturbed from natural variability of water vapour and clouds compared to the troposphere. This is because (a) the dependence of the equilibrium temperature of the stratosphere on CO_2 is larger than that of tropospheric temperature, (b) the equilibrium temperature of the stratosphere depends little upon tropospheric water vapour variability and (c) the influence of cloudiness upon equilibrium temperature is more pronounced in the troposphere than in the stratosphere where the influence decreases with height (Manabe and Weatherald, 1967). Furthermore, anthropogenic aerosols are mainly spread within the lower troposphere (He et al., 2008), and presumably have little effect on stratospheric temperatures.

Another open question is if the lower stratosphere started cooling since the time a reasonable global network became available i.e. after the international geophysical year (IGY) in 1957–1958. Such a long lasting cooling from the 60s until today needs to be re-examined and explained. To what extent are the cooling trends in the lower stratosphere related to human induced climate change? Has it been accelerating, for instance at high latitudes in winter/spring due to ozone depletion? Has it been interrupted by major volcanic eruptions and El Nino events (Zerefos et al., 1992) or large climatological anomalies?

The study addresses those questions and presents a new look at observed temperature trends over the Northern Hemisphere based on layer mean temperatures from thickness which are expected to improve homogeneity in both space and time and

ACPD
14, 1073–1112, 2014

reduce trend uncertainties before and after the 1980s in the lower stratosphere. Furthermore the tropopause variability and trends are also investigated with regard to the observed temperature trends and variability in the lower stratosphere and the troposphere.

2 Data and analysis of the statistical methods

2.1 Data

Tropospheric and stratospheric data used in this study are based on the following sources: (a) the NCEP/NCAR reanalysis I product (NCEP) data from 1958 to 2011 (Kalnay et al., 1996; Kistler et al., 2001), (b) the Free University of Berlin (FU-Berlin) from 1958 to 2001, (c) the Radiosonde Innovation Composite Homogenization (RICH) data (Haimberger, 2007; Haimberger et al., 2008) from 1958 to 2006 and (d) historical simulations with the NCAR Community Earth System Model (CESM) coupled to the "high-top" Whole Atmosphere Community Climate Model (WACCM) CESM1-WACCM (Marsh et al., 2013) from 1958 to 2005. Our analysis is focused at the Northern Hemisphere, as the data coverage in the pre-satellite era has been denser there than at the Southern Hemisphere.

Randel et al. (2009) pointed out that the sparse observational database and known instrumental uncertainties for the pre-satellite era, suggest an overall poor knowledge of trends for the period 1958–1978. Furthermore large differences and continuity problems are evident in the middle and upper stratosphere in the reanalysis data sets, implying that trend analysis of stratospheric temperatures for the whole time period of the reanalyses products should be considered with caution (WMO, 2011).

Aware of these problems, we opted to use here not the NCEP product of stratospheric temperature derived at specific atmospheric pressure levels, but rather the layer-mean temperature derived from the thickness of stratospheric and tropospheric layers (based on the geopotential height differences between specific atmospheric

ACPD
14, 1073–1112, 2014

pressure levels). Differences of monthly mean geopotential heights were used at standard atmospheric levels to derive the layer thickness and subsequently the layer mean temperature. Long-term global data sets of layer-mean temperatures derived from the geopotential height thickness from the troposphere to the stratosphere were chosen instead of mean temperatures because the approximate geostrophic balance of the upper winds in the free troposphere ensures that the contour analysis of the layers is more representative than the temperature analysis alone. For these reasons the thickness is well suited for an investigation of large-scale climatic fluctuations of temperature.

For the NCEP dataset we have used the layers 1000–925 hPa (planetary boundary layer), 925–500 hPa (free troposphere), 500–300 hPa (upper troposphere), 100–50 hPa and 50–30 hPa (lower stratosphere). The layer-mean temperatures were then used to calculate the averaged layer mean temperature over the latitude belts: northern polar (90–60° N), northern mid-latitudes (60–30° N) and the northern tropics (30–5° N). Furthermore, we also used in our analysis the tropopause pressure from NCEP to sudy the interannual correlation of tropopause pressure with tropospheric and stratospheric temperatures.

The FU-Berlin stratospheric analysis data set is based on subjective hand analyses of temperature and geopotential height for the Northern Hemisphere, derived from daily radiosonde observations, and thicknesses derived from TOVS (operationally transmitted SATEMs) over data sparse regions. Hydrostatic and geostrophic balances were assumed, and observed winds were used to guide the height and temperature analyses. The analyses are provided as gridded data sets with a horizontal resolution of $10^\circ \times 10^\circ$ before 1973, and $5^\circ \times 5^\circ$ thereafter. FU-Berlin geopotential height data are available from July 1957 until December 2001 at 100, 50, and 30 hPa (Labitzke et al., 2002). Hence, from the FU-Berlin dataset we calculated, following the same procedure as with the NCEP dataset, layer-mean temperatures for the two lower stratospheric layers, 100–50 hPa and 50–30 hPa. The RICH dataset was used at the standard atmospheric levels.

ACPD
14, 1073–1112, 2014

Evidence for an earlier greenhouse cooling effect

C. S. Zerefos et al.

In our analysis we have used simulations with CESM1-WACCM, a state-of-the-art "high top" chemistry climate model coupled to the earth system model CESM that extends from the surface to 5.1×10^{-6} hPa (approximately 140 km). It has 66 vertical levels and horizontal resolution of 1.9° latitude by 2.5° longitude. The historical simulations with CESM1-WACCM were carried out as part of phase 5 of the Coupled Model Intercomparison Project (CMIP5). CESM1-WACCM has an active ocean and sea ice components as described by Holland et al. (2012). As shown in Marsh et al. (2013) for CESM1-WACCM, an updated parameterization of non-orographic gravity waves led to an improvement in the frequency of Northern Hemisphere (NH) sudden stratospheric warmings (SSWs). Furthermore the model also includes a representation of the QBO leading to a significant improvement in the representation of ozone variability in the tropical stratosphere compared to observations. The model's chemistry module is based on version 3 of the Model for OZone And Related chemical Tracers (Kinnison et al., 2007). Volcanic aerosol surface area density in WACCM is prescribed from a monthly zonal mean time series derived from observations including the following major volcanic eruptions in historical simulations: Krakatau (1883), Santa Maria (1902), Agung (1963), El Chichón (1982), and Pinatubo (1991). WACCM explicitly represents the radiative transfer of the greenhouse gases CO_2, CH_4, N_2O, H_2O, CFC-12 and CFC-11 (which includes also additional halogen species). WACCM simulation used here was performed with all observed forcing from 1955–2005.The observed forcing included changes in surface concentrations of radiatively active species, daily solar spectral irradiance, volcanic sulphate heating and the QBO. A more detailed description of the CESM1-WACCM historical simulations can be found in Marsh et al. (2013).

As each source of analysis/reanalysis data spans over a different period, the time series were deseasonalized for the period of 1961–1990, common to all data sets. The same procedure was followed for the tropopause pressure. The temperature anomalies from the RICH dataset available at standard pressure levels were adjusted accordingly.

ACPD
14, 1073–1112, 2014

2.2 Analysis of methods

A multiple linear regression time series analysis with an autoregressive statistical model is applied on the deseasonalized time series of zonally averaged layer mean temperature similarly to the statistical approach applied by Reinsel et al. (2005). The regression model is of the form:

$$M_t = \alpha_0 + \alpha_1 Tr_t + \Sigma giZi + N_t; \quad 0 < t \le T \tag{1}$$

Where M_t is the monthly deseasonalized zonal mean temperature.

The terms included account for linear trends (Tr_t). The terms $giZi$ in the statistical model reflect the temperature variability related to the natural variability, where Zi represent a number of climatic and dynamical indices and gi are the respective regression coefficients. Specifically the climatic and dynamical indices used here include the 11 yr solar cycle (using the solar F10.7 radio flux as a proxy), plus two orthogonal time series to model QBO, namely the standardized zonal wind at 30 hPa and 50 hPa (e.g., Crooks and Gray, 2005; Austin et al., 2009).

It is well known that significant transient warming events occurred in the stratosphere following the volcanic eruptions of Agung (March 1963), El Chichon (April 1982) and Mt. Pinatubo (June 1991), and these can substantially influence temperature trend estimates (especially if the volcanic events occur near either end of the time series in question). The common approach in order to avoid a significant influence on trend results is to omit data for 2 yr following each eruption in the regression analysis. In order to investigate the role played by stratospheric aerosols, we include terms to account for the influence of stratospheric aerosol variability, using the Stratospheric Aerosol Optical Depth (Sato et al., 1993) as an index in the regression model.

Finally, N_t is the unexplained noise term. The statistical model is first-order autoregressive (AR(1)), and the term N_t satisfies:

$$Nt = \varphi N_{t-1} + et \tag{2}$$

ACPD
14, 1073–1112, 2014

where *et* is an independent random variable with zero mean, commonly known as the white noise residuals. This AR(1) model allows for the noise to be (auto)correlated among successive measurements and is typically positive for data which show smoothly varying changes (naturally occurring) in Nt over time (Reinsel, 2002).

The temperature trends and the role played by the various climatic and dynamic factors described above are examined in detail. The focus is on the detection of trends before and after the beginning of the satellite era (i.e. 1979), a period that is also the benchmark for ozone depletion.

3 Results

3.1 Summer and year-round trends

In the summer, the stratosphere is less disturbed because it is characterised by lower vertically propagating wave activity from the troposphere, it has smaller natural variability than winter (Webb, 1966; Berger and Lübken, 2011; Gettelman et al., 2011) and it is also not influenced by chemical ozone depletion due to ODSs at high latitudes. Hence the less "noisy" summer records offer the opportunity to investigate for better estimates of the lower stratospheric temperature trends. Figure 1 presents the time series of the layer mean temperatures in summer (June–July–August) for the Northern Hemisphere at tropical, mid and higher latitudinal zones from the lower troposphere up to the stratosphere, calculated from NCEP reanalysis, FU-Berlin and RICH datasets. The thick black lines represent the linear trends before and after 1980, a year that marks the beginning of the availability of satellite data whose inclusion resulted to increased global coverage. Figure 1 shows a consistent cooling of the lower stratosphere in NCEP, FU-Berlin and RICH datasets that persists in both pre- and post-80s periods. Specifically, for the period 1958–1979, there is a cooling trend for the whole Northern Hemisphere of $-0.58 \pm 0.17\,^{\circ}\mathrm{C\,decade}^{-1}$ in NCEP, $-0.30 \pm 0.16\,^{\circ}\mathrm{C\,decade}^{-1}$ in RICH and $-0.48 \pm 0.20\,^{\circ}\mathrm{C\,decade}^{-1}$ in FU-Berlin. For the common post-1980s pe-

ACPD
14, 1073–1112, 2014

riod (1980–2001), the respective trends are $-0.79 \pm 0.18\,^{\circ}\mathrm{C\,decade}^{-1}$ in NCEP, $-0.66 \pm 0.16\,^{\circ}\mathrm{C\,decade}^{-1}$ for RICH and $-0.82 \pm 0.19\,^{\circ}\mathrm{C\,decade}^{-1}$ in FU-Berlin. The CESM1-WACCM model results agree with re-analysis and the observations, indicating a persistent cooling of the lower stratosphere during summer for the whole Northern Hemisphere by $-0.33 \pm 0.17\,^{\circ}\mathrm{C\,decade}^{-1}$ for 1958–1979 and by $-0.35 \pm 0.20\,^{\circ}\mathrm{C\,decade}^{-1}$ for 1980–2001. However the modelled trends are generally lower than re-analysis and observations. We should point that our analysis was also performed for the ERA-40 dataset (not shown here) with the trend results for the two periods (1958–1979 and 1980–2001) being similar to NCEP trend results.

The summertime lower stratosphere trends at the different latitudinal belts (see Table 1 and Tables SMT1 and SMT2 in the Supplement) indicate generally statistically significant (at 95 %) cooling trends over both pre-1980s and post-1980s periods in the tropics (5–30° N) and mid-latitudes (30–60° N) based on NCEP, FU-Berlin and RICH datasets which is also reproduced by CESM1-WACCM (Table 2). However, in polar regions (60–90° N), the lower stratosphere cooling trends are either non-statistically significant or marginally significant at the 95 % confidence level for NCEP, FU-Berlin and RICH datasets. The same result is also indicated in CESM1-WACCM simulation (Table 2).

In the lower northern hemispheric troposphere (1000–500 hPa), non-statistically significant (at 95 %) trends or slight cooling trends prevail in the period 1958–1979 (0.06 ± 0.06 for NCEP and $-0.12 \pm 0.06\,^{\circ}\mathrm{C\,decade}^{-1}$ for RICH) followed by significant warming trends over the period 1980–2005 ($0.25 \pm 0.05\,^{\circ}\mathrm{C\,decade}^{-1}$ for both NCEP and RICH). CESM1-WACCM shows a persistent warming of the lower troposphere during summer by $0.21 \pm 0.17\,^{\circ}\mathrm{C\,decade}^{-1}$ in the pre-1980s period and $0.21 \pm 0.14\,^{\circ}\mathrm{C\,decade}^{-1}$ in the post-80s period. However, when excluding the polar latitudes, CESM1-WACCM shows a non-statistically significant (at 95 %) trend in the period 1958–1979 ($0.04 \pm 0.12\,^{\circ}\mathrm{C\,decade}^{-1}$) followed by a warming trend over the period 1980–2005 ($0.22 \pm 0.11\,^{\circ}\mathrm{C\,decade}^{-1}$) in agreement with NCEP and RICH.

ACPD
14, 1073–1112, 2014

The NCEP tropopause pressure follows closely (but in reverse) the tropospheric temperature long term change with tropopause pressure increasing in the pre-1980s period (tropopause height decreases) and decreasing in the post-80s period (tropopause height increases) at all three latitude zones. It should be pointed out that the increasing trend of tropopause pressure over the tropics in the pre-80s period is small and not statistically significant at 95 % level. The summer CESM1-WACCM tropopause pressure trends (Table 2) generally agree within 1-sigma with the respective NCEP trends (Table 1) with exception for the mid-latitudes of the pre-1980s period where CESM1-WACCM shows a statistical significant decreasing trend (tropopause height increases).

The year-round temperature and tropopause trends (Fig. 2) generally show similar results to those derived for the summer period (see also Tables SMT3, SMT4, SMT5 and SMT6 in the Supplement). In the lower stratosphere, the layer mean temperatures are decreasing continuously from late 1950s and throughout the records onwards. Specifically, for the period 1958–1979, there is a cooling trend for the whole Northern Hemisphere of $-0.58 \pm 0.08\,^{\circ}\mathrm{C\,decade}^{-1}$ in NCEP, $-0.33 \pm 0.08\,^{\circ}\mathrm{C\,decade}^{-1}$ in RICH and $-0.44 \pm 0.10\,^{\circ}\mathrm{C\,decade}^{-1}$ in FU-Berlin. For the common for all datasets period 1980–2001, the respective trends are $-0.76 \pm 0.09\,^{\circ}\mathrm{C\,decade}^{-1}$ in NCEP, $-0.64 \pm 0.08\,^{\circ}\mathrm{C\,decade}^{-1}$ for RICH and $-0.71 \pm 0.10\,^{\circ}\mathrm{C\,decade}^{-1}$ in FU-Berlin. The CESM1-WACCM model shows also a persistent cooling of the lower stratosphere by $-0.40 \pm 0.09\,^{\circ}\mathrm{C\,decade}^{-1}$ for 1958–1979 and by $-0.24 \pm 0.10\,^{\circ}\mathrm{C\,decade}^{-1}$ for 1980–2001.The decreasing trends of lower stratospheric temperatures are statistically significant (at 95 % confidence level) at the tropical belt (5–30° N) and the mid-latitudes (30–60° N) for all datasets. For the polar latitudes (60–90° N), it should be noted the non-statistically significant (95 %) small negative temperature (or even positive) trend during the pre-1980s period at the lower stratosphere in both RICH and FU-Berlin datasets in contrast to NCEP and CESM1-WACCM. For the post-1980s period in the lower stratosphere over polar latitudes all datasets indicate statistically significant cooling trends but with the tension in CESM1-WACCM simulation for a smaller cooling trend.

ACPD
14, 1073–1112, 2014

In the lower troposphere over the Northern Hemisphere, an insignificant change or a small cooling trend from the beginning of our datasets through the end of 1970s, (0.01 ± 0.03 for NCEP and $-0.13 \pm 0.03\,^{\circ}\mathrm{C\,decade}^{-1}$ for RICH) is followed by a statistically significant warming trend in the post-1980s period (0.30 ± 0.02 for NCEP and $0.27 \pm 0.02\,^{\circ}\mathrm{C\,decade}^{-1}$ for RICH). CESM1-WACCM shows a persistent warming of the lower troposphere during summer by $0.23 \pm 0.09\,^{\circ}\mathrm{C\,decade}^{-1}$ in the pre-1980s period and $0.28 \pm 0.07\,^{\circ}\mathrm{C\,decade}^{-1}$ in the post-80s period. Tropospheric temperature trends in CESM1-WACCM simulations (see Supplement SMT6) generally agree within 1-sigma with NCEP temperature trends before and after the 1980s with exception the pre-1980s trend in polar latitudes showing a statistical significant warming in contrast to NCEP and RICH datasets. When excluding the polar latitudes, CESM1-WACCM shows a non-statistically significant (at 95 %) trend in the period 1958–1979 (0.05 ± 0.06) followed by a warming trend over the period 1980–2005 ($0.24 \pm 0.06\,^{\circ}\mathrm{C\,decade}^{-1}$) in agreement with NCEP and RICH.

3.2 Monthly trends

The temperature trends were also calculated on a monthly basis. The layer mean temperature trends based on NCEP reanalysis (Fig. 3) are persistently negative at the lower stratosphere for all months, for both periods before and after 1979 at the tropical and mid-latitude latitudinal belts. The monthly temperature trends based on the RICH dataset (Fig. 4) and the FU-Berlin dataset (Fig. 5) also show persistent negative temperature trends in the lower stratosphere for all months for both periods before and after 1979 at the tropical and mid-latitude latitudinal belts in agreement with NCEP. The CESM1-WACCM simulation reproduces the cooling trends in the lower stratosphere for both pre-1980s and post-1980s at the tropical and mid-latitude latitudinal belts (Fig. 6).

At the polar latitudes, we also find cooling trends for all months in NCEP, except in March–April with a characteristic feature of an abrupt shift from a negative trend in winter to a positive trend in early spring for the pre-1980s (Fig. 3e). In the post-80s period the cooling trends are seen in all months (except January and February)

ACPD
14, 1073–1112, 2014

maximizing in March–April which may be associated to the Arctic ozone depletion by ODSs (Fig. 3f). In the lower stratosphere over polar latitudes for the pre-80s period, both RICH (Fig. 4e) and FU-Berlin (Fig. 5a and c) datasets do not show statistically significant (95 %) negative trends, in contrast to NCEP. However, it should be noted that the abrupt shift from a negative trend in winter to a positive trend in early spring is a common feature in all three datasets. In the post-80s period both RICH and FU-Berlin datasets indicate cooling trends maximizing in early spring in agreement with the NCEP results presumably due to the ozone depletion issue within the Arctic polar vortex. The CESM1-WACCM simulation captures at polar latitudes (Fig. 6e) the shift from a negative trend in winter to a positive trend in early spring for the pre-80s period but the winter cooling trends are much stronger than in NCEP, RICH and FU-Berlin datasets. In the post-80s period the cooling trends are seen in all months (except February and March) maximizing in April but the spring cooling trend is smaller than in NCEP, RICH and FU-Berlin datasets (Fig. 6f). Overall, all datasets indicate that persistent cooling trends in the lower stratosphere exist in all months and for both periods before and after 1979 which is a robust feature over the tropical belt and the middle latitudes.

3.3 Tropopause – temperature correlation

As seen in Figs. 1 and 2, the tropopause pressure follows closely (but reversed) the tropospheric temperature long-term course with a cooling trend or absence of a trend until about the end of the 1970s and a warming trend from about the mid-1980s until present. Moving up in the lower stratosphere, we have seen that all datasets show persistent cooling temperature trends for both the pre-1980s and post-1980s periods (Figs. 1 and 2). In this section we investigate the interannual correlation of temperature with tropopause pressure on a monthly basis with the aim of unraveling the relative contribution of tropospheric and stratospheric temperatures on the interannual and long-term variability of tropopause pressure. As has been pointed out in previous studies, the interannual variability and the trends in tropopause height are mainly determined

ACPD
14, 1073–1112, 2014

by the interannual variability and the trends of temperature in the lower stratosphere and upper troposphere (Seidel et al., 2006; Son et al., 2009).

At the tropical latitudinal belt (5–30° N) the pearson correlation between tropopause pressure and layer mean temperature (based on NCEP reanalysis) is negative at the troposphere ranging from −0.3 to −0.7 becoming positive and stronger at the lower stratosphere ranging from 0.6 to 0.9 (Fig. 7a). The negative correlations in the troposphere have a seasonal signal with the tendency to get stronger during the summer period while in the lower stratosphere the strong positive correlation persists throughout the course of the year. Hence it is inferred from Fig. 7a that throughout the year the interannual variance of the lower stratospheric temperatures contribute to the interannual variability at the tropopause region, a higher percentage than that contributed from the variance of tropospheric temperatures. The relative contribution of tropospheric temperatures in the interannual variance at tropopause maximizes during the warm period of the year. CESM1-WACCM (Fig. 7d) reproduces fairly well the correlation pattern of NCEP at the tropical band, thus indicating good skill of the model to simulate the relation in the interannual variability between tropopause height and temperature in the lower stratosphere/upper troposphere.

At mid-latitudes, the tropopause-temperature correlations in NCEP dataset become weaker, reaching 0.4 at the lower stratosphere and −0.5 at the troposphere mainly from June to September (Fig. 7b) indicating a higher sensitivity of tropopause interannual changes to tropospheric temperature changes during the warm season. CESM1-WACCM (Fig. 7e) captures the basic pattern of the tropopause-temperature correlations seen in NCEP for mid-latitudes.

At polar latitudes (60–90° N), the negative correlations (in NCEP) in the troposphere have a seasonal signal with the tendency to get stronger during the warm period of the year reaching a value of −0.7 while in the lower stratosphere the positive correlations become stronger during the cold part of the year reaching a value of 0.8 (Fig. 7c). Thus the interannual variability of lower stratospheric temperature dominates over tropospheric temperature for controlling the interannual variability of the tropopause dur-

ACPD
14, 1073–1112, 2014

ing the cold part of the year linked with the development of the polar vortex. In contrast during the warm period of the year, the interannual variability of tropospheric temperature takes over stratospheric temperature, linked to the higher heating rates of the polar troposphere.

The tropopause–temperature correlations pattern in CESM1-WACCM over the polar latitudes (Fig. 7f) is similar to the pattern of mid-latitudes and does not capture the NCEP correlation pattern of polar latitudes. A common feature for the three latitudinal belts and for both NCEP and WACCM is that the negative correlations in the troposphere have a seasonal signal with the tension to get stronger during the warm part of the year, linked to the more efficient mechanism of tropospheric heating to affect the interannual variability of climate variables at the tropopause region.

4 Discussion and concluding remarks

The analysis is mainly based on monthly layer mean temperatures derived from geopotential height thicknesses between specific pressure levels that improve homogeneity in both space and time and reduce uncertainties in the trend analysis. After removing natural related variability with the use of climatic and dynamical indices in a autoregressive multiple regression model, the calculated year-round trends showed persistent decreasing temperature trends in the lower stratosphere before and after 1980s. This is also confirmed from the trend analyses in summer when the stratosphere is less disturbed, the Brewer–Dobson circulation is weaker and it is also not influenced at high latitudes by the chemical ozone depletion due to ODSs found in the winter–early spring period (e.g. Harris et al., 2008).These decreasing lower stratosphere trends are robust features for NCEP, FU-Berlin and RICH datasets in the tropics and the middle latitudes. The CESM1-WACCM simulation reproduces the lower stratosphere cooling trends temperature trends before and after the 1980s in the tropics and over mid-latitudes, consistent with an increased infrared emission by CO_2 (Marsh et al., 2013). However, the lower stratosphere modelled trends are generally lower than re-analysis

ACPD
14, 1073–1112, 2014

and the observations. This result is in agreement with the study of Santer et al. (2013) who showed that on average the CMIP5 models analyzed underestimate the observed cooling of the lower stratosphere maybe due to the need for a more realistic treatment of stratospheric ozone depletion and volcanic aerosol forcing.

It should be pointed that the temperature long-term trends based on RICH are within 1-sigma of the thickness calculated layer temperature trends from FU-Berlin and NCEP datasets indicating a consistent picture for the cooling trend of the lower stratosphere before and after the 1980s. The consistency of RICH temperature trends with the thickness calculated layer mean temperature trends from FU-Berlin and NCEP, enhances our confidence for the cooling trend in the lower stratosphere in the pre-satellite era despite the documented trend uncertainties of the radiosonde datasets during this period (Randel and Wu, 2006; Free and Seidel, 2007; Randel et al., 2009). Furthermore the inspection of lower stratospheric trends on a monthly basis for all datasets indicate the persistent cooling trends in the lower stratosphere to be a common feature for all months before and after 1980s both at the tropical belt and over the middle latitudes.

The post-1980s lower stratosphere cooling is a common finding in the global mean based on all available satellite and radiosonde datasets while the stratosphere cooling is also reported for the pre-satellite era since 1958 (WMO, 2011; Zerefos and Mantis, 1977). These long term cooling trends in the lower stratosphere can be maintained by increasing GHGs that cool the stratosphere while warming the troposphere (IPCC, 2007 and references therein; Polvani and Solomon, 2012). The post 1980s decrease in stratospheric ozone in late winter-early spring at mid and polar latitudes of Northern Hemisphere due to ODSs complicates the issue (Harris et al., 2008). However the persistency of the cooling trends in our results in the lower stratosphere for all months and especially during the less disturbed summer period before and after the 1980s over the tropics and the mid-latitudes indicates that the anthropogenic enhanced greenhouse effect is the most plausible cause for the observed stratospheric cooling in the Northern Hemisphere.

ACPD
14, 1073–1112, 2014

At polar latitudes (60–90° N), though, the lower stratosphere cooling trends are either non-statistically significant or marginally significant at the 95 % confidence level for all datasets. This finding could be related to the competing dynamical and radiative processes that may reduce the statistical significance of these trends. A number of modeling studies suggest that the greenhouse warming leads to stronger tropical upwelling and stronger Brewer–Dobson (BD) circulation (Rind et al., 2001; Cordero and Forster, 2006; Butchart et al., 2006, 2010; Austin and Li, 2006; Rosenlof and Reid, 2008; Garcia and Randel, 2008; Lamarque and Solomon, 2010). The GHG induced strengthening of BD circulation may lead to a relatively warmer lower stratosphere at higher latitudes thus masking the GHGs radiatively cooling. In contrast, over the tropics both dynamical and radiative processes act towards the same direction, cooling the lower stratosphere. Our results are in line with other recent studies. For example, Thompson and Solomon (2009) demonstrated that the contrasting latitudinal structures of recent stratospheric temperature (i.e., stronger cooling in the tropical lower stratosphere than in the extratropics) and ozone trends (i.e., enhanced ozone reduction in the tropical lower stratosphere) are consistent with the assumption of increases in the stratospheric overturning BD circulation. Free (2011) also pointed that the trends in the tropical stratosphere show an inverse relationship with those in the Arctic for 1979–2009, which might be related to changes in stratospheric circulation.

In the troposphere, a common feature in the RICH and NCEP datasets is a non-statistically significant trend or a slight cooling trend until about the end of the 1970s, followed by a warming trend until the present day for the three latitudinal belts. This pre-1980s cooling trend (or absence of trend) in the troposphere is associated with a notable cooling trend from the late 1940s to 1970s (IPCC, 2007), which has been raised as a point of weakness against the advocates of the theory of CO_2 related anthropogenic global warming (Thompson et al., 2010). However, apart from the important role of the decadal natural variability hampering the anthropogenic climate change (Ring et al., 2012; Kosaka and Xie, 2013), anthropogenic aerosols also attracted the scientific interest as a possible cause for this mid-century cooling due to a high concen-

ACPD
14, 1073–1112, 2014

tration of sulphate aerosols emitted in the atmosphere by industrial activities and volcanic eruptions during this period causing the so-called "solar dimming" effect (e.g. Wild et al., 2007; Zerefos et al., 2012). Hence the pre-1980s small cooling trend or insignificant change might be due to natural variability in the ocean-atmosphere system in combination with the compensating role of anthropogenic aerosols in the troposphere. Concerns have been raised recently that increases in aerosol from anthropogenic air pollution and associated dimming of surface solar radiation could have masked to a large extent the temperature rise induced by increasing greenhouse gases, so that the observed temperature records would not reflect the entire dimension of greenhouse warming (Andreae et al., 2005; Wild et al., 2007).

The investigation of the interannual correlation of tropopause pressure with tropospheric and stratospheric temperatures showed a few distinct characteristics. A common feature for the three latitudinal belts in both NCEP and CESM1-WACCM is that the influence of tropospheric temperature on the interannual variability of tropopause has a seasonal signal with the tendency to get stronger during the warm period of the year when the tropospheric heating maximizes.

In the tropics (5–30° N), the interannual variability of lower stratospheric temperature dominates over tropospheric temperature for controlling the interannual variability of the tropopause throughout the year in both NCEP and CESM1-WACCM. This could possibly explain why at the tropical zone (5–30° N) there is a decreasing trend of tropopause pressure (increase of tropopause height) in the pre-1980s. Seidel and Radel (2006) also reported using radiosonde data that on the multidecadal scale for tropical atmosphere, the tropopause height change is more sensitive to stratospheric temperature change than tropospheric change and hence at the lowest frequencies the tropopause is primarily coupled with stratospheric temperatures.

At mid-latitudes the tropopause pressure – temperature correlations become generally weaker maximizing from June to September with tropospheric temperatures slightly overwhelming stratospheric temperatures for the control of the interannual variability of tropopause. This is in line with the study of Son et al. (2009) who analysed a set of

ACPD
14, 1073–1112, 2014

long-term integrations with stratosphere-resolving chemistry climate models (CCMs) and reported that at mid-latitudes the linear tropopause height increase is rather controlled by the upper troposphere warming rather than the lower stratosphere cooling. Wu et al. (2013) reported a significant positive correlation between the changes in the tropospheric temperature induced by aerosols and tropopause height at mid-latitudes, the zone between 30° and 60° in both hemispheres. Hence taking into account the anthropogenic aerosols variability in the troposphere, the tropopause trends at mid-latitudes may not solely reflect human induced climate change signal from GHGs.

At polar latitudes (in NCEP) the interannual variability of lower stratospheric temperature dominates over tropospheric temperature for controlling the interannual variability of the tropopause during the cold part of the year (linked with the development of the polar vortex) while the opposite occurs during the warm period of the year (linked to the higher heating rates of polar troposphere). However, during the late winter-early spring, chemical ozone depletion within polar Arctic stratosphere in the post-1980s period could further cool the lower stratosphere (in addition to the radiative effect of GHGs) leading possibly to an even higher tropopause. The GHGs induced strengthening of BD circulation, which leads to a relatively warmer lower stratosphere (thus masking the GHGs radiatively cooling) and lower tropopause, further complicates the issue of using lower stratosphere temperature and tropopause height as climate change indicators at polar latitudes. CESM1-WACCM at polar latitudes does not capture the respective NCEP correlation pattern, an issue that needs further investigation.

The relative contribution of lower stratosphere vs. troposphere for the control of tropopause low frequency variability is an important issue for understanding past and future tropopause trends in view also of the monotonically increasing future tropopause height trends till the end of 21st century predicted by both stratosphere-resolving chemistry climate models (CCMs) and the Intergovernmental Panel on Climate Change Fourth Assessment Report (AR4) models (Son et al., 2009).

In conclusion, we provide additional evidence for an early greenhouse cooling signal of the lower stratosphere before the 1980s, which appears earlier than the tropo-

ACPD
14, 1073–1112, 2014

spheric greenhouse warming signal possibly due to the compensating role of antropogenic aerosols. As a result, it may be that the stratosphere could have provided an early warning of human-produced climate change. In line with the theoretical expectations that equilibrium temperature in the stratosphere compared to the troposphere is more sensitive to anthropogenic GHGs and less sensitive to tropospheric water vapour, aerosols and clouds, it is tentatively proposed that the stratosphere is more suitable for the detection of man-made climate change signal. We suggest that the maintenance and enrichment of the ground-based and satellite global networks for monitoring stratospheric temperatures and the tropopause region, which adds value in understanding the behaviour of the interface between the troposphere and stratosphere, are essential steps to unravel the issue of future human induced climate change signals.

Supplementary material related to this article is available online at http://www.atmos-chem-phys-discuss.net/14/1073/2014/acpd-14-1073-2014-supplement.pdf.

Acknowledgements. For University of Illinois, this research was supported in part from NASA under project NASA NNX12AF32G. We acknowledge the support provided by the Mariolopoulos-Kanaginis Foundation for the Environmental Sciences. Prodromos Zanis and Juerg Luterbacher would like also to acknowledge the support in the framework of the Greece–Germany Exchange and Cooperation Programme, IKYDA 2012.

References

Andreae, M. O., Jones, C. D., and Cox, P. M.: Strong present-day aerosol cooling implies a hot future, Nature, 435, 1187–1190, doi:10.1038/nature03671, 2005.

Angell, J. K. and Korshover, J.: Global temperature variations in the troposphere and stratosphere, 1958–1982, Mon. Weather Rev., 111, 901–921, 1983.

Austin, J. and Li, F.: On the relationship between the strength of the Brewer–Dobson circulation and the age of stratospheric air, Geophys. Res. Lett., 33, L17807, doi:10.1029/2006GL026867, 2006.

Austin, J., Wilson, R. J., Akiyoshi, H., Bekki, S., Butchart, N., Claud, C., Fomichev, V. I., Forster, P., Garcia, R. R., Gillett, N. P., Keckhut, P., Langematz, U., Manzini, E., Nagashima, T., Randel, W. J., Rozanov, E., Shibata, K., Shine, K. P., Struthers, H., Thompson, D. W. J., Wu, F., and Yoden, S.: Coupled chemistry climate model simulations of stratospheric temperatures and their trends for the recent past, Geophys. Res. Lett., 36, L13809, doi:10.1029/2009GL038462, 2009.

Berger, U. and Lübken, F.-J.: Mesospheric temperature trends at midlatitudes in summer, Geophys. Res. Lett., 38, L22804, doi:10.1029/2011GL049528, 2011.

Butchart, N., Scaife, A. A., Bourqui, M., de Grandpré, J., Hare, S. H. E., Kettleborough, J., Langematz, U., Manzini, E., Sassi, F., Shibata, K., Shindell, D., and Sigmond, M.: Simulations of anthropogenic change in the strength of the Brewer–Dobson circulation, Clim. Dynam., 27, 727–741, doi:10.1007/s00382-006-0162-4, 2006.

Butchart, N., Cionni, I., Eyring, V., Shepherd, T. G., Waugh, D. W., Akiyoshi, H., Austin, J., Brhl, C., Chipperfield, M. P., Cordero, E., Dameris, M., Deckert, R., Dhomse, S., Frith, S. M., Garcia, R. R., Gettelman, A., Giorgetta, M. A., Kinnison, D. E., Li, F., Mancini, E., McLandress, C., Pawson, S., Pitari, G., Plummer, D. A., Rozanov, E., Sassi, F., Scinocca, J. F., Shibata, K., Steil, B., and Tian, W.: Chemistry-climate model simulations of twenty-first century stratospheric climate and circulation change, J. Climate, 23, 5349–5374, doi:10.1175/2010JCLI3404.1, 2010.

Christy, J. R., Spencer, R. W., Norris, W. B., Braswell, W. D., and Parker, D. E.: Error estimates of version 5.0 of MSU-AMSU bulk atmospheric temperatures, J. Atmos. Ocean. Tech., 20, 613–629, 2003.

Cordero, E. C. and Forster, P. M. de F.: Stratospheric variability and trends in models used for the IPCC AR4, Atmos. Chem. Phys., 6, 5369–5380, doi:10.5194/acp-6-5369-2006, 2006.

Crooks, S. A. and Gray, L. J.: Characterization of the 11 year solar signal using a multiple regression analysis of the ERA-40 dataset, J. Climate, 18, 996–1015, 2005.

Engel, A., Möbius, T., Bönisch, H., Schmidt, U., Heinz, R., Levin, I., Atlas, E., Aoki, S., Nakazawa, T., Sugawara, S., Moore, F., Hurst, D., Elkins, J., Schauffler, S., Andrews, A., and Boering, K.: Age of stratospheric air unchanged within uncertainties over the past 30 years, Nat. Geosci., 2, 28–31, doi:10.1038/ngeo388, 2009.

Free, M.: The seasonal structure of temperature trends in the tropical lower Stratosphere, J. Climate, 24, 859–866, doi:10.1175/2010JCLI3841.1, 2011.

Free, M. and Lanzante, J.: Effect of volcanic eruptions on the vertical temperature profile in radiosonde data and climate models, J. Climate, 22, 2925–2939, doi:10.1175/2008JCLI2562.1, 2009.

Free, M. and Seidel, D. J.: Comments on “Biases in Stratospheric and Tropospheric temperature trends derived from historical radiosonde data”, J. Climate, 20, 3704–3709, doi:10.1175/JCLI4210.1, 2007.

Free, M., Seidel, D. J., Angell, J. K., Lanzante, J., Durre, I., and Peterson, T. C.: Radiosonde Atmospheric Temperature Products for Assessing Climate (RATPAC): a new data set of large-area anomaly time series, J. Geophys. Res., 110, D22101, doi:10.1029/2005JD006169, 2005.

Fioletov, V. E.: Estimating the 27 day and 11 year solar cycle variations in tropical upper stratospheric ozone, J. Geophys. Res., 114, D02302, doi:10.1029/2008JD010499, 2009.

Fu, Q., Solomon, S., and Lin, P.: On the seasonal dependence of tropical lower-stratospheric temperature trends, Atmos. Chem. Phys., 10, 2643–2653, doi:10.5194/acp-10-2643-2010, 2010.

Garcia, R. R. and Randel, W. J.: Acceleration of the Brewer–Dobson circulation due to increases in greenhouse gases, J. Atmos. Sci., 65, 2731–2739, doi:10.1175/2008JAS2712.1, 2008.

Gettelman, A., Hoor, P., Pan, L. L., Randel, W. J., Hegglin, M. I., and Birner, T.: The extratropical upper troposphere and lower stratosphere, Rev. Geophys., 49, RG3003, doi:10.1029/2011RG000355, 2011.

Haimberger, L.: Homogenization of radiosonde temperature time series using innovation statistics, J. Climate, 20, 1377–1403, doi:10.1175/JCLI4050.1, 2007.

Haimberger, L., Tavolato, C., and Sperka, S.: Toward elimination of the warm bias in historic radiosonde temperature records—Some new results from a comprehensive intercomparison of upper-air data, J. Climate, 21, 4587–4606, doi:10.1175/2008JCLI1929.1, 2008.

Harris, N. R. P., Kyrö, E., Staehelin, J., Brunner, D., Andersen, S.-B., Godin-Beekmann, S., Dhomse, S., Hadjinicolaou, P., Hansen, G., Isaksen, I., Jrrar, A., Karpetchko, A., Kivi, R., Knudsen, B., Krizan, P., Lastovicka, J., Maeder, J., Orsolini, Y., Pyle, J. A., Rex, M., Vanicek, K., Weber, M., Wohltmann, I., Zanis, P., and Zerefos, C.: Ozone trends at north-

ern mid- and high latitudes – a European perspective, Ann. Geophys., 26, 1207–1220, doi:10.5194/angeo-26-1207-2008, 2008.
He, Q., Li, C., Mao, J., Lau, A. K.-H., and Chu, D. A.: Analysis of aerosol vertical distribution and variability in Hong Kong, J. Geophys. Res., 113, D14211, doi:10.1029/2008JD009778, 2008.
Holland, M. M., Bailey, D. A., Briegleb, B. P., Light, B., and Hunke, E.: Improved sea ice shortwave radiation physics in CCSM4: the impact of melt ponds and aerosols on Arctic Sea Ice, J. Climate, 25, 1413–1430, doi:10.1175/JCLI-D-11-00078.1, 2012.
Hu, Y. and Fu, Q.: Stratospheric warming in Southern Hemisphere high latitudes since 1979, Atmos. Chem. Phys., 9, 4329–4340, doi:10.5194/acp-9-4329-2009, 2009.
IPCC, Climate Change 2007: The Physical Science Basis. Contribution of Working Group I to the Fourth Assessment, Report of the Intergovernmental Panel on Climate Change, edited by: Solomon, S., Qin, D., Manning, M., Chen, Z., Marquis, M., Averyt, K. B., Tignor, M., and Miller, H. L., Cambridge University Press, Cambridge, UK and New York, NY, USA, 996 pp., 2007.
IPCC, Climate Change 2013: The Physical Science Basis. Contribution of Working Group I to the Fifth Assessment Report (AR5) of the Intergovernmental Panel on Climate, available at: http://www.climatechange2013.org/ (last access: October 2013), 2013.
Iwasaki, T., Hamada, H., and Miyazaki, K.: Comparisons of Brewer–Dobson circulations diagnosed from reanalyses, J. Meteorol. Soc. Jpn., 87, 997–1006, doi:10.2151/jmsj.87.997, 2009.
Johanson, C. M. and Fu, Q.: Antarctic atmospheric temperature trend patterns from satellite observations, Geophys. Res. Lett., 34, L12703, doi:10.1029/2006GL029108, 2007.
Kalnay, E., Kanamitsu, M., Kistler, R., Collins, W., Deaven, D., Gandin, L., Iredell, M., Saha, S., White, G., Woollen, J., Zhu, Y., Leetmaa, A., Reynolds, R., Chelliah, M., Ebisuzaki, W., Higgins, W., Janowiak, J., Mo, K. C., Ropelewski, C., Wang, J., Jenne, R., and Joseph, D.: The NCEP/NCAR 40 year Reanalysis Project, B. Am. Meteorol. Soc., 77, 437–471, 1996.
Kawatani, Y. and Hamilton, K.: Weakened stratospheric quasibiennial oscillation driven by increased tropical mean upwelling, Nature, 497, 478–481, doi:10.1038/nature12140, 2013.
Kinnison, D. E., Brasseur, G. P., Walters, S., Garcia, R. R., Marsh, D. R., Sassi, F., Harvey, V. L., Randall, C. E., Emmons, L., Lamarque, J. F., Hess, P., Orlando, J. J., Tie, X. X., Randel, W., Pan, L. L., Gettelman, A., Granier, C., Diehl, T., Niemeier, U., and Simmons, A. J.: Sensi-

ACPD
14, 1073–1112, 2014

tivity of chemical tracers to meteorological parameters in the MOZART-3 chemical transport model, J. Geophys. Res., 112, D20302, doi:10.1029/2006JD007879, 2007.
Kistler, R., Kalnay, E., Collins, W., Saha, S., White, G., Woollen, J., Chelliah, M., Ebisuzaki, W., Kanamitsu, M., Kousky, V., van den Dool, H., Jenne, R., and Fiorino, M.: The NCEP-NCAR 50 year Reanalysis: monthly means CD-ROM and documentation, B. Am. Meteorol. Soc., 82, 247–267, 2001.
Kosaka, Y. and Xie, S. P.: Recent global-warming hiatus tied to equatorial Pacific surface cooling, Nature, 501, 403–407, doi:10.1038/nature12534, 2013.
Labitzke, K. and Coauthors: The Berlin Stratospheric Data Series, Meteorological Institute, Free University Berlin, CD-ROM, 2002.
Lamarque, J.-F., and Solomon, S.: Impact of changes in climate and halocarbons on recent lower stratospheric ozone and temperature trends, J. Climate, 23, 2599–2611, doi:10.1175/2010JCLI3179.1, 2010.
Lin, P., Fu, Q., Solomon, S., and Wallace, J. M.: Temperature trend patterns in Southern Hemisphere high latitudes: novel indicators of stratospheric changes, J. Climate, 22, 6325–6341, doi:10.1175/2009JCLI2971.1, 2009.
Manabe, S. and Weatherald, R. T.: Thermal equilibrium of the atmosphere with a given distribution of relative humidity, J. Atmos. Sci., 24, 241–259, 1967.
Marsh, D. R., Mills, M. J., Kinnison, D. E., Lamarque, J.-F., Calvo, N., and Polvani, L. M.: Climate change from 1850 to 2005 simulated in CESM1(WACCM), J. Climate, 26, 7372–7391, doi:10.1175/JCLI-D-12-00558.1, 2013.
Mears, C. A. and Wentz, F. J.: Construction of the Remote Sensing Systems V3.2 atmospheric temperature records from the MSU and AMSU microwave sounders, J. Atmos. Ocean. Technol., 26, 1040–1056, doi:10.1175/2008JTECHA1176.1, 2009.
Miller, A. J., Nagatani, R. M., Tiao, G. C., Niu, X. F., Reinsel, G. C., Wuebbles, D., and Grant, K.: Comparisons of observed ozone and temperature trends in the lower stratosphere, Geophys. Res. Lett., 19, 929–932, 1992.
Polvani, L. M. and Solomon, S.: The signature of ozone depletion on tropical temperature trends, as revealed by their seasonal cycle in model integrations with single forcings, J. Geophys. Res., 117, D17102, doi:10.1029/2012JD017719, 2012.
Randel, W. J. and Thompson, A. M.: Interannual variability and trends in tropical ozone derived from SAGE II satellite data and SHADOZ ozonesondes, J. Geophys. Res., 116, D07303, doi:10.1029/2010JD015195, 2011.

ACPD
14, 1073–1112, 2014

Randel, W. J. and Wu, F.: Biases in stratospheric and tropospheric temperature trends derived from historical radiosonde data, J. Climate, 19, 2094–2104, 2006.
Randel, W. J., Shine, K. P., Austin, J., Barnett, J., Claud, C., Gillet, N. P., Keckhut, P., Langematz, U., Lin, R., Long, C., Mears, C., Miller, A., Nash, J., Seidel, D. J., Thompson, D. W. J., Wu, F., and Yoden, S.: An update of observed stratospheric temperature trends, J. Geophys. Res., 114, D02107, doi:10.1029/2008JD010421, 2009.
Ramaswamy, V., Schwarzkopf, M. D., Randel, W. J., Santer, B. D., Soden, B. J., and Stenchikov, G. L.: Anthropogenic and natural influences in the evolution of lower stratospheric cooling, Science, 311, 1138–1141, doi:10.1126/science.1122587, 2006.
Reinsel, G. C.: Trend analysis of upper stratospheric Umkehr ozone data for evidence of turnaround, Geophys. Res. Lett., 29, 1451, doi:10.1029/2002GL014716, 2002.
Reinsel, G. C., Miller, A. J., Weatherhead, E. C., Flynn, L. E., Nagatani, R. M., Tiao, G. C., and Wuebbles, D. J.: Trend analysis of total ozone data for turnaround and dynamical contributions, J. Geophys. Res., 110, D16306, doi:10.1029/2004JD004662, 2005.
Rind, D., Lerner, J., and McLinden, C.: Changes of tracer distributions in the doubled CO_2 climate, J. Geophys. Res., 106, 28061–28079, 2001.
Ring, M. J., Lindner, D., Cross, E. M., and Schlesinger, M. E.: Causes of the Global Warming observed since the 19th century, Atmospheric and Climate Sciences, 2, 401–415, doi:10.4236/acs.2012.24035, 2012.
Rosenlof, K. H. and Reid, G. C.: Trends in the temperature and water vapor content of the tropical lower stratosphere: sea surface connection, J. Geophys. Res., 113, D06107, doi:10.1029/2007JD009109, 2008.
Santer, B. D., Hnilo, J. J., Wigley, T. M. L., Boyle, J. S., Doutriaux, C., Fiorino, M., Parker, D. E., and Taylor, K. E.: Uncertainties in observationally based estimates of temperature change in the free atmosphere, J. Geophys. Res., 104, 6305–6333, doi:10.1029/1998JD200096, 1999.
Santer, B. D., Sausen, R., Wigley, T. M. L., Boyle, J. S., AchutaRao, K., Doutriaux, C., Hansen, J. E., Meehl, G. A., Roeckner, E., Ruedy, R., Schmidt, G., and Taylor, K. E.: Behavior of tropopause height and atmospheric temperature in models, reanalyses, and observations: decadal changes, J. Geophys. Res., 108, 4002, doi:10.1029/2002JD002258, 2003a.
Santer, B. D., Wehner, M. F., Wigley, T. M. L., Sausen, R., Meehl, G. A., Taylor, K. E., Ammann, C., Arblaster, J., Washington, W. M., Boyle, J. S., and Brüggemann, W.: Contributions of anthropogenic and natural forcing to recent tropopause height changes, Science, 301, 479–483, doi:10.1126/science.1084123, 2003b.

ACPD
14, 1073–1112, 2014

Santer, B. D., Painter, J. F., Mears, C. A., Doutriaux, C., Caldwell, P., Arblaster, J. M., Cameron-Smith, P. J., Gillett, N. P., Gleckler, P. J., Lanzante, J., Perlwitz, J., Solomon, S., Stott, P. A., Taylor, K. E., Terray, L., Thorne, P. W., Wehner, M. F., Wentz, F. J., Wigley, T. M. L., Wilcox, L. J., and Zou, C.: Identifying human influences on atmospheric temperature, P. Natl. Acad. Sci. USA, 110, 26–33, 2013.

Sato, M., Hansen, J. E., McCormick, M. P., and Pollack, J. B.: Stratospheric aerosol optical depth, 1850–1990, J. Geophys. Res., 98, 22987–22994, 1993.

Seidel, D. J. and Randel, W. J.: Variability and trends in the global tropopause estimated from radiosonde data, J. Geophys. Res., 111, D21101, doi:10.1029/2006JD007363, 2006.

Sherwood, S. C., Meyer, C. L., Allen, R. J., and Titchner, H. A.: Robust tropospheric warming revealed by iteratively homogenized radiosonde data, J. Climate, 21, 5336–5350, doi:10.1175/2008JCLI2320.1, 2008.

Shine, K. P., Bourqui, M. S., Forster, P. M. de F., Hare, S. H. E., Langematz, U., Braesicke, P., Grewe, V., Ponater, M., Schnadt, C., Smith, C. A., Haigh, J. D., Austin, J., Butchart, N., Shindell, D. T., Randel, W. J., Nagashima, T., Portmann, R. W., Solomon, S., Seidel, D. J., Lanzante, J., Klein, S., Ramaswamy, V., and Schwarzkopf, M. D.: A comparison of model-simulated trends in stratospheric temperatures, Q. J. Roy. Meteor. Soc., 129, 1565–1588, doi:10.1256/qj.02.186, 2003.

Son, S.-W., Polvani, L. M., Waugh, D. W., Birner, T., Akiyoshi, H., Garcia, R. R., Gettelman, A., Plummer, D. A., and Rozanov, E.: The impact of stratospheric ozone recovery on tropopause height trends, J. Climate, 22, 429–445, doi:10.1175/2008JCLI2215.1, 2009.

Staehelin, J., Harris, N. R. P., Appenzeller, C., and Eberhard, J.: Ozone trends: a review, Rev. Geophys., 39, 231– 290, 2001.

Tiao, G. C., Reinsel, G. C., Xu, D., Pedrick, J. H., Zhu, X., Miller, A. J., DeLuisi, J. J., Mateer, C. L., Wuebbles, D. J.: Effects of autocorrelation and temporal sampling schemes on estimates of trend and spatial correlation, J. Geophys. Res., 95, 20507–20517, 1990.

Thompson, D. W. J. and Solomon, S.: Recent stratospheric climate trends as evidenced in radiosonde data: Global structure and tropospheric linkages, J. Climate, 18, 4785–4795, 2005.

Thompson, D. W. J. and Solomon, S.: Understanding recent stratospheric climate change, J. Climate, 22, 1934–1943, doi:10.1175/2008JCLI2482.1, 2009.

ACPD
14, 1073–1112, 2014

Thompson, D. W. J., Wallace, J. M., Kennedy, J. J., and Jones, P. D.: An abrupt drop in Northern Hemisphere sea surface temperature around 1970, Nature, 467, 444–447, doi:10.1038/nature09394, 2010.
Thompson, D. W. J., Seidel, D. J., Randel, W. J., Zou, C.-Z., Butler, A. H., Mears, C., Osso, A., Long, C., and Lin, R.: The mystery of recent stratospheric temperature trends, Nature, 491, 692–697, doi:10.1038/nature11579, 2012.
Thorne, P. W., Parker, D. E., Tett, S. F. B., Jones, P. D., McCarthy, M., Coleman, H., and Brohan, P.: Revisiting radiosonde upper air temperatures from 1958 to 2002, J. Geophys. Res., 110, D18105, doi:10.1029/2004JD005753, 2005.
Webb, W. L.: Structure of the stratosphere and mesosphere, Academic Press, New York and London, 380 pp., 1966.
Wild, M., Ohmura, A., and Makowski, K.: Impact of global dimming and brightening on global warming, Geophys. Res. Lett., 34, L04702, doi:10.1029/2006GL028031, 2007.
WMO (World Meteorological Organization), Scientific Assessment of Ozone Depletion: 2010, Global Ozone Research and Monitoring Project–Report No. 52, Geneva, Switzerland, 516 pp., 2011.
WMO (World Meteorological Organization), Scientific Assessment of Ozone Depletion: 2006, Global Ozone Research and Monitoring Project–Report No. 50, Geneva, Switzerland, 572 pp., 2007.
Wu, J., Xu, Y, Yang, Q., Han, Z., Zhao, D., and Tang, J.: A numerical simulation of aerosols' direct effects on tropopause height, Theor. Appl. Climatol., 112, 659–671, doi:10.1007/s00704-012-0760-5, 2013.
Zerefos, C. S. and Mantis, H. T.: Climatic fluctuations in the Northern Hemisphere stratosphere, Arch. Met. Geoph. Biokl. Ser. B, 25, 33–39, 1977.
Zerefos, C. S., Bais, A. F., Ziomas, I. C., and Bojkov, R. D.: On the relative importance of quasi-biennial oscillation and El Nino/southern oscillation in the revised Dobson total ozone records, J. Geophys. Res., 97, 10135–10144, doi:10.1029/92JD00508, 1992.
Zerefos, C. S., Tourpali, K., Eleftheratos, K., Kazadzis, S., Meleti, C., Feister, U., Koskela, T., and Heikkilä, A.: Evidence of a possible turning point in solar UV-B over Canada, Europe and Japan, Atmos. Chem. Phys., 12, 2469–2477, doi:10.5194/acp-12-2469-2012, 2012.
Zou, C.-Z., Gao, M., and Goldberg, M. D.: Error structure and atmospheric temperature trends in observations from the Microwave Sounding Unit, J. Climate, 22, 1661–1681, doi:10.1175/2008JCLI2233.1, 2009.

ACPD
14, 1073–1112, 2014

Table 1. Trend calculations in Northern Hemisphere summer (JJA) based on the monthly normalised time series of the layer mean temperature (°C decade^{-1}) and tropopause pressure (hPa decade^{-1}) calculated from NCEP reanalysis and filtered from natural variations at the latitudinal belts (a) 5–30° N, (b) 30–60° N and (c) 60–90° N. The layers are: L1: 1000–925 hPa, L2: 925–500 hPa, L3: 500–300 hPa, L4: 100–50 hPa and L5: 50–30 hPa. The trends calculations refer to the periods 1958–1979, 1980–2001, 1980–2005 and 1980–2011.

Period 1958–1979						
	90–60° N		60–30° N		30–05° N	
Layer	Trend	*t* test	Trend	*t* test	trend	*t* test
L1	0.26 ± 0.11	2.48	−0.01 ± 0.04	−0.25	0.11 ± 0.03	3.91
L2	0.10 ± 0.09	1.12	−0.11 ± 0.04	-2.92	−0.01 ± 0.04	−0.22
L3	−0.42 ± 0.07	−5.69	−0.25 ± 0.04	-6.89	−0.11 ± 0.05	−2.19
L4	−0.57 ± 0.31	−1.83	−0.59 ± 0.06	-10.37	−0.21 ± 0.12	−1.79
L5	−0.77 ± 0.35	−2.19	−0.74 ± 0.09	-8.38	−0.59 ± 0.10	−5.99
TP	**1.98 ± 1.25**	**1.58**	**2.42 ± 0.28**	**8.57**	**0.19 ± 0.24**	**0.78**
Period 1980–2001						
	90–60° N		60–30° N		30–05° N	
Layer	Trend	*t* test	Trend	*t* test	trend	*t* test
L1	0.39 ± 0.11	3.42	0.23 ± 0.04	5.31	0.06 ± 0.03	2.00
L2	0.05 ± 0.09	0.56	0.19 ± 0.04	4.74	0.04 ± 0.04	0.93
L3	0.14 ± 0.08	1.83	0.07 ± 0.04	1.50	−0.10 ± 0.05	−2.20
L4	−0.70 ± 0.34	−2.04	−0.94 ± 0.07	−14.14	−0.90 ± 0.11	−8.30
L5	−0.66 ± 0.36	−1.84	−0.83 ± 0.08	−10.02	−0.73 ± 0.09	−8.20
TP	**−1.87 ± 1.69**	**−1.10**	**−1.59 ± 0.35**	**−4.52**	**−0.82 ± 0.24**	**−3.43**
Period 1980–2005						
	90–60° N		60–30° N		30–05° N	
Layer	Trend	*t* test	Trend	*t* test	trend	*t* test
L1	0.61 ± 0.09	6.75	0.28 ± 0.03	8.31	0.11 ± 0.02	5.51
L2	0.14 ± 0.07	2.07	0.24 ± 0.03	7.81	0.11 ± 0.03	3.67
L3	0.23 ± 0.06	3.91	0.11 ± 0.03	3.20	−0.01 ± 0.03	−0.35
L4	−0.43 ± 0.26	−1.61	−0.69 ± 0.06	−11.86	−0.79 ± 0.08	−9.51
L5	−0.46 ± 0.28	−1.66	−0.63 ± 0.07	−9.14	−0.55 ± 0.08	−6.90
TP	**−1.06 ± 1.30**	**−0.82**	**−0.72 ± 0.27**	**−2.68**	**−0.75 ± 0.18**	**−4.14**
Period 1980–2011						
	90–60° N		60–30° N		30–05° N	
Layer	Trend	*t* test	Trend	*t* test	trend	*t* test
L1	0.65 ± 0.07	9.18	0.29 ± 0.03	10.83	0.13 ± 0.02	7.85
L2	0.25 ± 0.05	4.68	0.27 ± 0.03	10.50	0.16 ± 0.02	6.40
L3	0.28 ± 0.05	5.99	0.16 ± 0.03	5.91	0.07 ± 0.03	2.22
L4	−0.32 ± 0.22	−1.50	−0.53 ± 0.05	−10.03	−0.67 ± 0.07	−10.21
L5	−0.38 ± 0.22	−1.70	−0.45 ± 0.06	−7.59	−0.41 ± 0.06	−6.51
TP	**−1.49 ± 1.07**	**−1.40**	**−1.07 ± 0.25**	**−4.23**	**−0.91 ± 0.15**	**−5.92**

ACPD
14, 1073–1112, 2014

ACPD
14, 1073–1112, 2014

Evidence for an earlier greenhouse cooling effect

C. S. Zerefos et al.

Table 2. Trend calculations in Northern Hemisphere summer (JJA) based on the monthly normalised time series of the layer mean temperature (°C decade^{-1}) and tropopause pressure TP (hPa decade^{-1}) calculated from the WACCM model and filtered from natural variations at the latitudinal belts (a) 5–30° N, (b) 30–60° N and (c) 60–90° N. The layers are: L1: 1000–925 hPa, L2: 925–500 hPa, L3: 500–300 hPa, L4: 100–50 hPa and L5: 50–30 hPa. The trends calculations refer to the periods 1958–1979, 1980–2001 and 1980–2005.

Period 1958–1979						
	90–60° N		60–30° N		30–05° N	
Layer	Trend	*t* test	Trend	*t* test	trend	*t* test
L1	0.70 ± 0.45	1.55	0.01 ± 0.32	0.02	−0.02 ± 0.10	−0.16
L2	0.37 ± 0.09	4.23	−0.01 ± 0.04	−0.20	0.19 ± 0.02	8.66
L3	0.13 ± 0.06	2.14	0.02 ± 0.04	0.43	0.24 ± 0.03	7.83
L4	−0.26 ± 0.32	−0.81	−0.22 ± 0.10	−2.25	−0.30 ± 0.09	−3.22
L5	−0.28 ± 0.35	−0.80	−0.32 ± 0.13	−2.41	−0.57 ± 0.10	−5.80
TP	**0.33 ± 1.13**	**0.29**	**−1.42 ± 0.45**	**−3.14**	**−0.57 ± 0.53**	**−1.07**
Period 1980–2001						
	90–60° N		60–30° N		30–05° N	
Layer	Trend	*t* test	Trend	*t* test	trend	*t* test
L1	0.14 ± 0.42	0.33	0.12 ± 0.36	0.34	0.40 ± 0.10	3.97
L2	0.40 ± 0.10	3.90	0.29 ± 0.04	6.67	0.22 ± 0.04	5.14
L3	0.33 ± 0.07	4.64	0.26 ± 0.05	5.25	0.29 ± 0.07	4.31
L4	−0.43 ± 0.28	−1.50	−0.16 ± 0.14	−1.19	−0.31 ± 0.15	−2.08
L5	−0.35 ± 0.31	−1.13	−0.40 ± 0.17	−2.40	−0.44 ± 0.16	−2.73
TP	**−2.20 ± 1.02**	**−2.16**	**−0.75 ± 0.43**	**−1.74**	**−0.10 ± 0.53**	**−0.19**
Period 1980–2005						
	90–60° N		60–30° N		30–05° N	
Layer	Trend	*t* test	Trend	*t* test	trend	*t* test
L1	0.04 ± 0.32	0.12	−0.03 ± 0.29	−0.11	0.35 ± 0.08	4.43
L2	0.34 ± 0.08	4.40	0.31 ± 0.04	8.39	0.23 ± 0.03	7.49
L3	0.30 ± 0.06	5.39	0.32 ± 0.04	7.83	0.32 ± 0.05	6.46
L4	−0.52 ± 0.23	−2.30	−0.13 ± 0.10	−1.28	−0.23 ± 0.11	−2.14
L5	−0.46 ± 0.25	−1.85	−0.34 ± 0.13	−2.72	−0.30 ± 0.11	−2.62
TP	**−2.87 ± 0.86**	**−3.35**	**−0.69 ± 0.34**	**−2.01**	**−0.55 ± 0.40**	**−1.38**

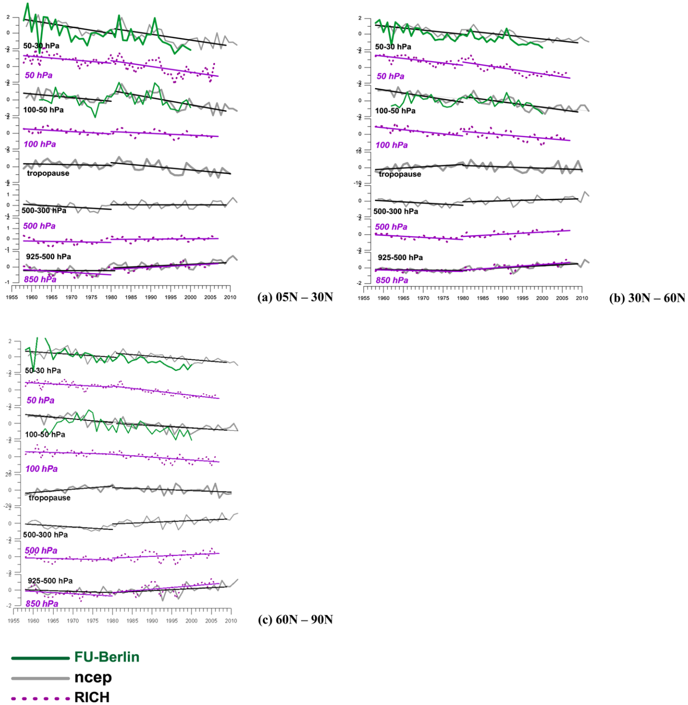

Fig. 1. Layer mean temperature variations in Northern Hemisphere summer (JJA) at layers 925–500 hPa, 500–300 hPa, 100–50 hPa and 50–30 hPa calculated from NCEP reanalysis and FU-Berlin datasets and filtered from natural variations for three latitudinal belts **(a)** 5–30° N, **(b)** 30–60° N and **(c)** 60–90° N. The respective summer normalised time series of temperature from RICH dataset at levels 850 hPa, 500 hPa, 50 hPa and 30 hPa are also illustrated as well as the NCEP tropopause pressure. The trends lines before and after 1979 are superimposed. Grey lines denote NCEP reanalysis variations. Green lines denote variations as depicted in the FU-Berlin analysis, while purple dotted lines the RICH data temperature.

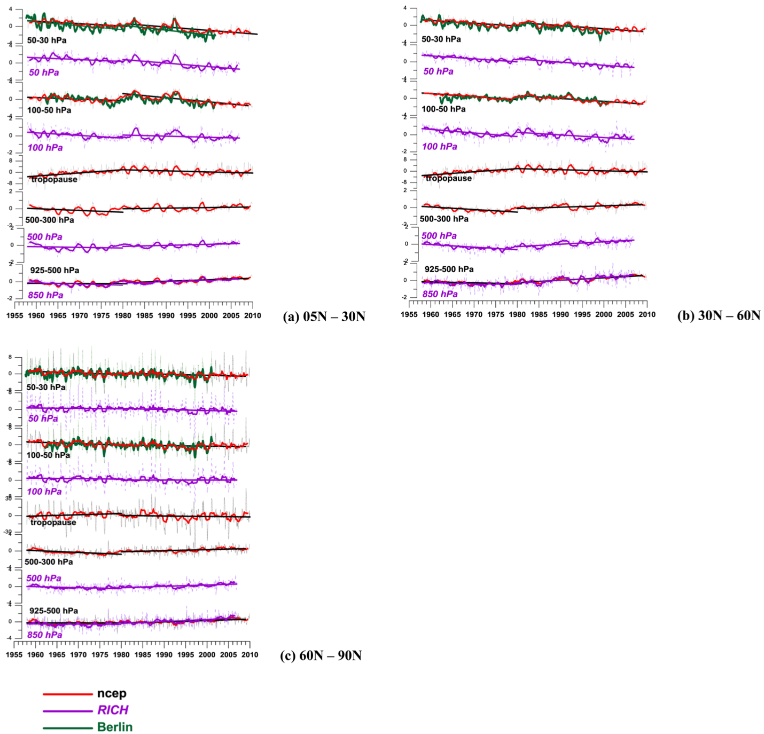

Fig. 2. Monthly normalised time series of the layer mean temperature at layers 925–500 hPa, 500–300 hPa, 100–50 hPa and 50–30 hPa calculated from NCEP reanalysis and FU-Berlin datasets for the Northern Hemisphere and filtered from natural variations at the latitudinal belts **(a)** 5–30° N, **(b)** 30–60° N and **(c)** 60–90° N. The respective monthly normalised time series of temperature from RICH dataset at levels 850 hPa, 500 hPa, 50 hPa and 30 hPa are also illustrated with purple lines as well as the NCEP tropopause pressure normalized monthly means. The trends lines before and after 1979 are also superimposed.

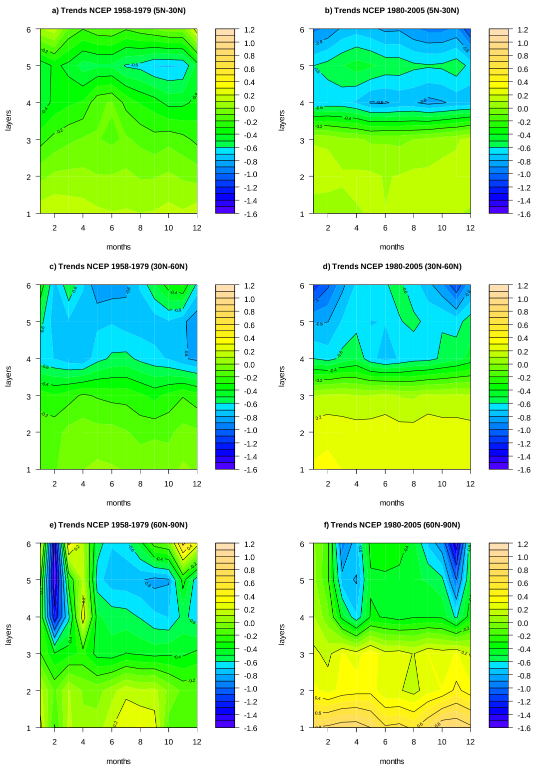

Fig. 3. Layer mean temperature trends (°C decade^{-1}) for each month (x axis) and layer (y axis) based on NCEP reanalysis over the periods 1958–1979 and 1980–2005, respectively, for three latitudinal belts **(a)** and **(b)** for 5–30° N, **(c)** and **(d)** for 30–60° N and **(e)** and **(f)** for 60–90° N. The layers are: Layer 1: 1000–925 hPa, Layer 2: 925–500 hPa, Layer 3: 500–300 hPa, Layer 4: 100–50 hPa, Layer 5: 50–30 hPa, and Layer 6: 30–10 hPa.

ACPD
14, 1073–1112, 2014

Evidence for an earlier greenhouse cooling effect

C. S. Zerefos et al.

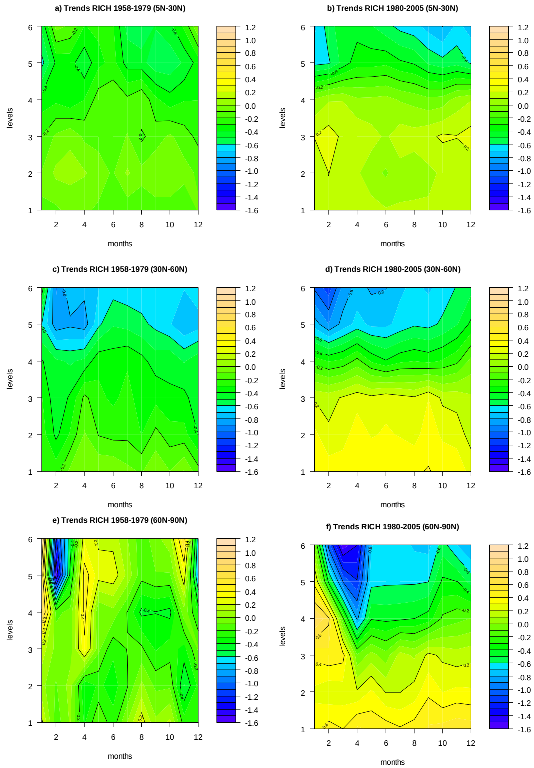

Fig. 4. Temperature trends (°C decade^{-1}) for each month (*x* axis) and level (*y* axis) based on RICH dataset over the periods 1958–1979 and 1980–2005, respectively, for three latitudinal belts **(a)** and **(b)** for 5–30° N, **(c)** and **(d)** for 30–60° N and **(e)** and **(f)** for 60–90° N. The levels are: Level 1: 850 hPa, Level 2: 500 hPa, Level 3: 300 hPa, Level 4: 100 hPa, Level 5: 50 hPa, and Level 6: 30 hPa.

ACPD

14, 1073–1112, 2014

Evidence for an earlier greenhouse cooling effect

C. S. Zerefos et al.

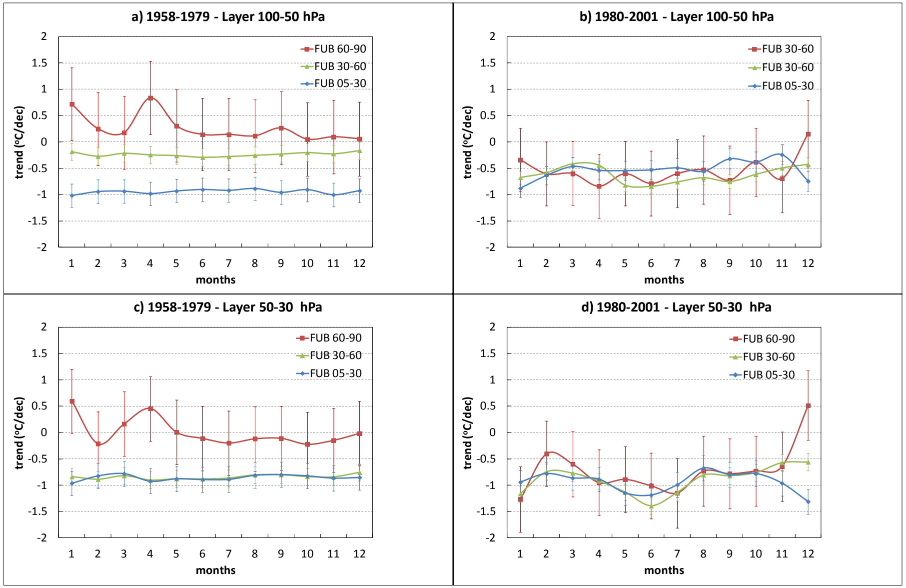

Fig. 5. Mean temperature trends (°C decade^{-1}) for each month (x axis) based on FU-Berlin dataset over the periods 1958–1979 and 1980–2001 for the layers 100–50 hPa (**a** and **b**) and 50–30 hPa (**c** and **d**) for the three latitudinal belts, 5–30° N (blue), 30–60° N (green) and 60–90° N (red).

ACPD
14, 1073–1112, 2014

Evidence for an earlier greenhouse cooling effect

C. S. Zerefos et al.

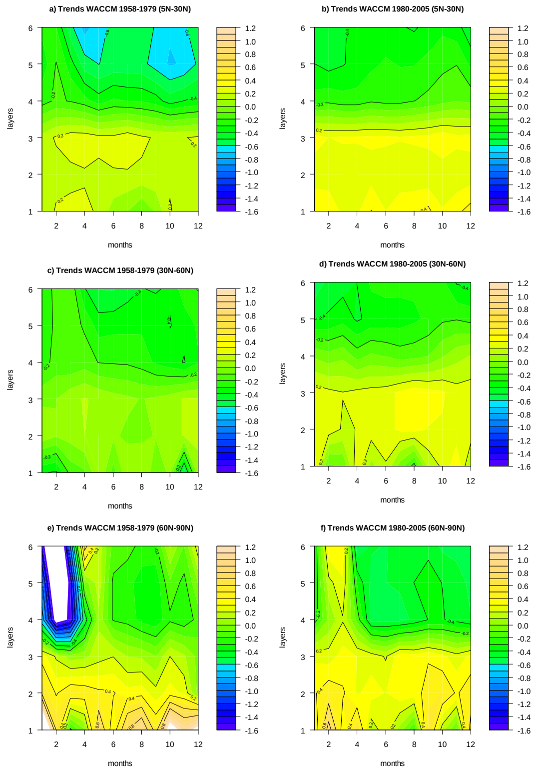

Fig. 6. Layer mean temperature trends (°C decade^{-1}) for each month (*x* axis) and layer (*y* axis) based on WACCM model over the periods 1958–1979 and 1980–2005, respectively, for three latitudinal belts **(a)** and **(b)** for 5–30° N, **(c)** and **(d)** for 30–60° N and **(e)** and **(f)** for 60–90° N. The layers are: Layer 1: 1000–925 hPa, Layer 2: 925–500 hPa, Layer 3: 500–300 hPa, Layer 4: 100–50 hPa, Layer 5: 50–30 hPa, and Layer 6: 30–10 hPa.

ACPD
14, 1073–1112, 2014

Evidence for an earlier greenhouse cooling effect

C. S. Zerefos et al.

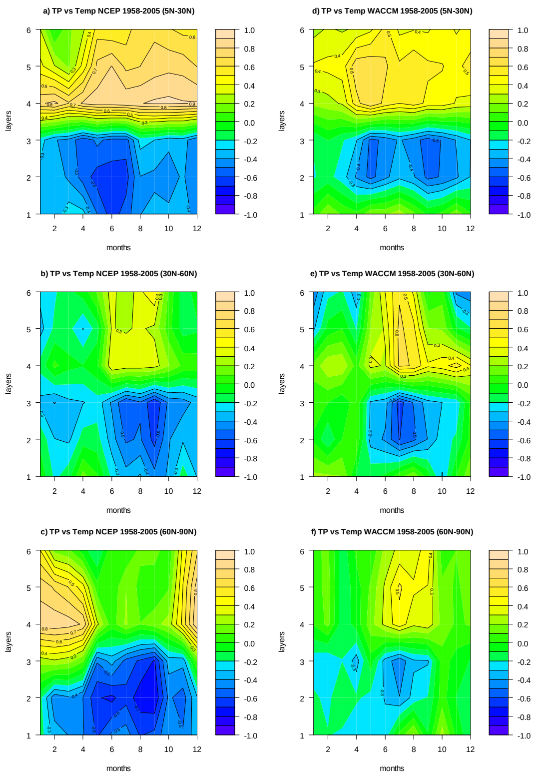

Fig. 7. Correlation plots between tropopause pressure and layer mean temperature for each month (*x* axis) and layer (*y* axis) based on NCEP reanalysis (left panel) and WACCM model (right panel) over the common period 1958–2005 for the three latitudinal belts: 5–30° N (**a** and **d**), 30–60° N (**b** and **e**) and 60–90° N (**c** and **f**). The layers are: Layer 1: 1000–925 hPa, Layer 2: 925–500 hPa, Layer 3: 500–300 hPa, Layer 4: 100–50 hPa, Layer 5: 50–30 hPa, and Layer 6: 30–10 hPa. The contours indicate the statistically significant correlations at 95 % significance level.

ACPD
14, 1073–1112, 2014